cAMP-PKA phosphorylation of tau confers risk for degeneration in aging association cortex

Becky C. Carlyle[a], Angus C. Nairn[a], Min Wang[b], Yang Yang[b], Lu E. Jin[b], Arthur A. Simen[a], Brian P. Ramos[a], Kelly A. Bordner[a], George E. Craft[a], Peter Davies[c], Mihovil Pletikos[b], Nenad Šestan[b], Amy F. T. Arnsten[b], and Constantinos D. Paspalas[b,1]

Departments of [a]Psychiatry and [b]Neurobiology, Yale University School of Medicine, New Haven, CT 06511; and [c]Litwin–Zucker Research Center for the Study of Alzheimer's Disease, Feinstein Institute for Medical Research, North Shore–Long Island Jewish Health System, Manhasset, NY 11030

The pattern of neurodegeneration in Alzheimer's disease (AD) is very distinctive: neurofibrillary tangles (NFTs) composed of hyperphosphorylated tau selectively affect pyramidal neurons of the aging association cortex that interconnect extensively through glutamate synapses on dendritic spines. In contrast, primary sensory cortices have few NFTs, even in late-stage disease. Understanding this selective vulnerability, and why advancing age is such a high risk factor for the degenerative process, may help to reveal disease etiology and provide targets for intervention. Our study has revealed age-related increase in cAMP-dependent protein kinase (PKA) phosphorylation of tau at serine 214 (pS214-tau) in monkey dorsolateral prefrontal association cortex (dlPFC), which specifically targets spine synapses and the Ca^{2+}-storing spine apparatus. This increase is mirrored by loss of phosphodiesterase 4A from the spine apparatus, consistent with increase in cAMP-Ca^{2+} signaling in aging spines. Phosphorylated tau was not detected in primary visual cortex, similar to the pattern observed in AD. We also report electron microscopic evidence of previously unidentified vesicular trafficking of phosphorylated tau in normal association cortex—in axons in young dlPFC vs. in spines in aged dlPFC—consistent with the transneuronal lesion spread reported in genetic rodent models. pS214-Tau was not observed in normal aged mice, suggesting that it arises with the evolutionary expansion of corticocortical connections in primates, crossing the threshold into NFTs and degeneration in humans. Thus, the cAMP-Ca^{2+} signaling mechanisms, needed for flexibly modulating network strength in young association cortex, confer vulnerability to degeneration when dysregulated with advancing age.

Aging is the highest risk factor for Alzheimer's disease (AD) (1), a neurodegenerative disorder that severely affects the association cortex. Neurofibrillary tangles (NFTs) are a hallmark of AD pathology (2), and their numbers correlate with cognitive decline (3). NFTs arise from phosphorylation of tau protein by a variety of kinases, including phosphorylation by cAMP-dependent protein kinase (PKA) at serine 214 (pS214-tau) (4) and at threonine 231 (pT231-tau) by a number of kinases, e.g., CaM kinase II, GSK-3, and cdk5 (5). Phosphorylation at S214 has synergistic actions when combined with other kinases, accelerating tau hyperphosphorylation at multiple sites (6). Hyperphosphorylation induces aggregation and then fibrillation, which in humans can progress to NFT formation. In AD, NFTs are selective to the association cortex (7, 8), where they specifically target pyramidal cells with the most extensive corticocortical connections (9). For example, layer III pyramidal cells of the dorsolateral prefrontal association cortex (dlPFC) have extensive corticocortical connections and are afflicted early and severely in AD (9). In contrast, primary sensory cortices (e.g., visual area V1) have very few NFTs even in late-stage disease (7, 8). Although this pattern of degeneration has been recognized for decades, it has not been known why extensively interconnected pyramidal cells in association cortex are selectively afflicted and why advancing age is such a high risk factor for their degeneration. These questions are key

to revealing disease etiology and thus developing strategies for intervention. Although rodent AD models have provided a wealth of information regarding β-amyloid (Aβ) and tau signaling, they have not addressed this important issue, as rodents lack highly developed association cortices, and genetic alterations are introduced throughout the cortex and do not mimic the pattern of pathology seen in humans (10).

Contrary to rodents, nonhuman primates have well-developed association cortices with many similarities to those of humans. Studies in the monkey have shown that layer III dlPFC pyramidal cell circuits generate the mental representations needed for abstract thought (11). Within and across these cognitive circuits, pyramidal cells excite each other through NMDA receptor (NMDAR) glutamate synapses on long thin spines (12). dlPFC synapses are modulated differently from those in V1, with permissive nicotinic-α7 receptor activation of NMDAR (13) and feedforward cAMP-Ca^{2+}-K^+ channel signaling to gate network inputs (14). In dendritic spines, internal Ca^{2+} is buffered by the spine apparatus (SA), the extension and elaboration of the smooth endoplasmic reticulum (SER) into the spine head. Stimulation of inositol trisphosphate receptors (IP3Rs) (15) and ryanodine receptors (RyRs) on the SA releases Ca^{2+}, a process amplified by cAMP-PKA signaling. For example, cAMP-PKA signaling increases internal Ca^{2+} release by increasing the efficacy and expression of IP3Rs (16) and by increasing Ca^{2+} leak through RyRs (17). Increased Ca^{2+} release can in turn promote

Significance

This study of the monkey cerebral cortex revealed age-related changes that help to answer key questions about Alzheimer's disease (AD): (*i*) why advancing age is the highest risk factor for AD and (*ii*) why neurofibrillary tangles (NFTs) in AD selectively target extensively interconnected pyramidal neurons in the highly evolved association cortex, but do not afflict the primary sensory cortex. NFTs arise from phosphorylation of tau protein. In aged prefrontal association cortex, we found increased cAMP-dependent protein kinase (PKA) phosphorylation of tau and corresponding loss of phosphodiesterase 4A, an enzyme that regulates cAMP-PKA signaling in dendritic spines where pyramidal neurons interconnect. In contrast, phosphorylated tau was not observed in aged primary visual cortex. These data provide new strategies for early intervention in AD.

cAMP production (18), fueling feedforward signaling (14). Ca^{2+}-cAMP-PKA signaling increases the open state of nearby K^+ channels (SK, HCN, KCNQ) on the spine membrane, which temporarily weakens synaptic efficacy, thus providing dynamic gating of network inputs to enhance mental flexibility and coordinate cognitive and arousal states (14) (see Fig. 6A). Importantly, feedforward Ca^{2+}-cAMP-PKA signaling receives negative feedback from phosphodiesterases (PDEs), e.g., PDE4s, which hydrolyze cAMP and terminate its actions (19). In particular, the isozyme PDE4A is prominent in dlPFC spines where corticocortical circuits interconnect (20).

It has been appreciated for many years that Ca^{2+} signaling is increased in the aging brain (21, 22) and that signs of increased cAMP-PKA signaling in aged PFC correlate with reduced neuronal firing and impaired cognition (23, 24). However, it has not been known why cAMP-PKA signaling becomes dysregulated with age and whether these changes contribute to vulnerability to degeneration. In recent years, "normal aging" and the "pathological aging" in AD have been studied as separate entities, even though advanced age is known to be the highest risk factor for degeneration. The study of the aging process in association cortex may reveal what renders its neurons particularly vulnerable and provide the much-needed bridge between "normal" and "pathological" aging. Here we used biochemistry, electron microscopy, and in vivo electrophysiology to examine the aging nonhuman primate association cortex. We report (i) loss of the cAMP-phosphodiesterase, PDE4A, and (ii) a concomitant increase of cAMP-PKA phosphorylation of tau, in dendritic spines where corticocortical circuits interconnect. The data help to explain the selective vulnerability of these highly evolved circuits with advancing age.

Results

Age-Related Increase in Tau Phosphorylation. We compared the expression of pS214-tau in young vs. aged monkeys and in young vs. aged mice. Immunocytochemistry against pS214-tau revealed extensive reactivity of layer III pyramidal cells in aged monkey dlPFC (Fig. 1A) but not in V1 (Fig. 1B), similar to the pattern of NFTs in AD. Immunoblots of heat-stable preparations demonstrated a highly significant correlation of pS214-tau expression in monkey dlPFC with increasing age ($r^2 = 0.9974$, $P = 0.00006$) as well as age-related reductions in soluble tau, consistent with increasing fibrillation (Fig. 1C and Fig. S1). Age-related increases were also observed at pT231-tau ($r^2 = 0.9808$, $P = 0.001$; Fig. 1C). In contrast to the aging monkey, there were only background levels of pS214-tau and no significant change with age in pT231-tau in mouse medial PFC (Fig. S2).

Given the prominence of pS214-tau in aged monkey dlPFC, we used immunoelectron microscopy (immunoEM) to determine its exact subcellular localization at a resolution that is not possible in postmortem human tissue. In young monkey dlPFC (Fig. 1D, Left), pS214-tau prevailed in axons and certain proximal pyramidal dendrites, with fine labeling along the microtubules. This contrasted with the aged dlPFC, where pS214-tau was heavily aggregated in dendrites over microtubule bundles (Fig. 1D, Right, and Fig. S3) and was especially prominent in spines (Fig. 1D, Lower). In aged spines, pS214-tau selectively accumulated at the postsynaptic membrane (Fig. 2 A and B) and the SA limiting membrane (Fig. 2 C–E). Importantly, pS214-tau was found only on asymmetric, presumed glutamatergic, axospinous synapses; symmetric, inhibitory synapses on spines (Fig. 2B) or synapses on dendrites (Fig. S3A) were not labeled. Thus, pS214-tau aggregates directly over aging NMDAR spine synapses where pyramidal cell circuits interconnect.

The optimally preserved monkey brain allowed direct visualization of p-tau trafficking in situ, i.e., a distinct association with endoplasmic vesicles and exo/endocytotic membrane profiles. In young dlPFC, pS214-tau–reactive vesicular profiles of 60 nm appeared exclusively in axons (Fig. 3 A and B) and particularly at axo-axonal appositions where they were observed to be fusing with the axolemma to form omega-shaped profiles (Fig. 3B). In
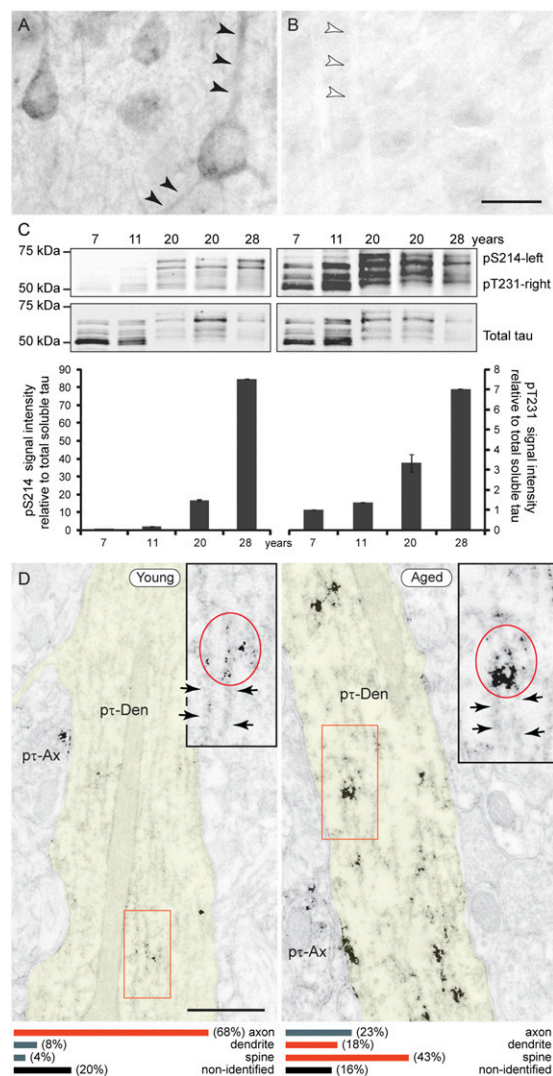
Fig. 1. Tau phosphorylation increases with age in monkey dlPFC. (A) The aged dlPFC (31 y) presents intense pS214-tau immunoreactivity along apical and basal pyramidal dendrites (arrowheads) and diffuse reactivity in the neuropil. (B) In contrast, pS214-tau is not detected in aged V1 (same hemisphere shown; arrowheads point to an apical dendrite for comparison). (Scale bar: 20 μm.) (C) Immunoblots of heat-stable tau preparations from dlPFC show an increase with age of tau phosphorylation at S214 (Left) and T231 (Right). (D) ImmunoEM demonstrates age-related aggregation of pS214-tau (red oval in Inset) along dendritic microtubules (arrows). Ax, axon; Den, dendrite. (Scale bars: 0.5 μm.) The bottom graphs summarize the distribution of pS214-tau in cellular profiles as the percentage of immunoreactive profiles in the neuropil of young vs. aged dlPFC (*SI Materials and Methods*).

aged dlPFC, pS214-tau–reactive vesicular profiles were no longer encountered in axons but found in spines instead, either fusing with the perisynaptic membrane flanking asymmetric, presumed glutamatergic synapses (Fig. 3C) or directly within the asymmetric synapse per se (Fig. 3D). Symmetric synapses on spines did not associate with p-tau–reactive vesicular profiles.

Age-Related Decrease in PDE4A. Why are dendritic spines in dlPFC a focus of pS214-tau accumulation with advancing age? Comparisons of young vs. aged monkey dlPFC indicate that increasing PKA phosphorylation of tau may involve age-related loss of PDE4A from spines, thus decreasing a key regulatory factor. In young dlPFC, PDE4A is prevalent in layer III spines, localized near the SA (Fig. 4 A and B) along with the PKA
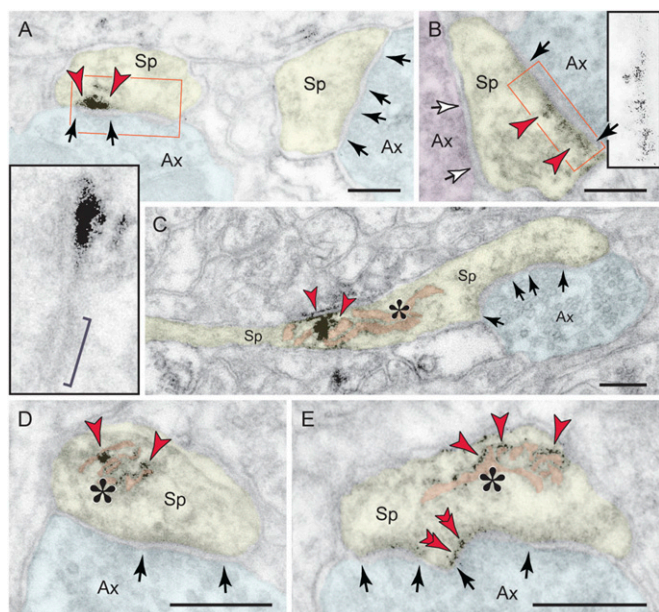
Fig. 2. Ultrastructural localization of pS214-tau in dendritic spines in monkey dlPFC. (*A* and *B*) In aged spines, p-tau (arrowheads) aggregates directly over the postsynaptic membrane of asymmetric, presumed glutamatergic synapses (black arrows and *Insets*); bracket in *A*, *Inset* denotes an asynaptic adherens junction for comparison. Symmetric synapses onto spines, as in synaptic triads, were not labeled (*B*, white arrows). (*C–E*) In addition to the selective accumulation at asymmetric spine synapses, p-tau in aged dlPFC aggregates over the SA (asterisk). Note that the limiting membrane of the apparatus reticular cisterns is labeled, as is the spine postsynaptic membrane in *E* (double arrowheads). Ax, axon; Sp, spine. (Scale bars: 200 nm.)

tethering A-kinase anchor protein 6 (AKAP6) (Fig. S4), where it is positioned to regulate feedforward cAMP-Ca^{2+} signaling. Quantitative immunoEM showed a selective loss of PDE4A from spines in aged monkey dlPFC (Fig. 4C). EM data were upheld by quantitative protein assay demonstrating significant decreases in the 105-kDa PDE4A subtype (equivalent to mouse PDE4A5) in aged monkey dlPFC (Fig. 5A). The protein data were consistent with physiological recordings from young vs. aged monkeys, where aged dlPFC neurons showed a blunted response to PDE4 inhibition (Fig. 5B and Fig. S5). Indeed, the firing patterns of aged neurons under control conditions resembled those of young neurons under conditions of reduced PDE4 activity. In summary, advancing age causes loss of PDE4A from spines, mirroring the location where pS214-tau accumulates in the aged dlPFC.

Similar but much subtler effects were observed in mouse medial PFC, with an age-related reduction of PDE4A5 protein in synapses (Fig. 5C and Fig. S6), which, however, was not evident in whole-tissue lysates (Fig. S7). Analysis of the rodent medial PFC also showed reduced PDE4A mRNA in aged mice (Fig. S8) and increased cAMP levels in aged rats: young (6 mo), 0.43 ± 0.045 (SEM) pmol/mg vs. aged (24 mo), 0.59 ± 0.02 (SEM) pmol/mg. Similar disinhibition of cAMP signaling in a large number of spines may increase PKA tau phosphorylation with advancing age. Finally, rolipram-mediated inhibition of PDE4 in mouse primary cortical neurons leads to increased PKA phosphorylation of tau on treatment with forskolin (Fig. 5D and Fig. S9), suggesting that loss of PDE4A in aged dlPFC spines could lead to pS214-tau accumulation in vivo.

Discussion

The current study revealed age-related increase in tau phosphorylation (pS214-tau and pT231-tau) and age-related reduction in PDE4A in pyramidal cell network synapses in primate association cortex (summarized in Fig. 6). As predicted with

reduced PDE4A expression, cAMP levels were increased in the aged PFC. These data are consistent with previous reports of increased pS133-cAMP response element-binding protein (pS133-CREB) in aged rodent PFC (23) and age-related increases in CREB-related genes in human association cortex (25). PDE4A loss from the SA suggests that loss of PDE4A regulation of cAMP may also contribute to increased Ca^{2+} signaling in aged dlPFC (21, 22), e.g., by increasing Ca^{2+} leak through RYRs (17). There were age-related increases in tau phosphorylation at T231, a site phosphorylated by multiple kinases, including several Ca^{2+}-activated kinases. More importantly, advancing age increased PKA phosphorylation of tau at S214, suggesting that dysinhibited cAMP contributes to vulnerability to degeneration in aged primate dlPFC. pS214-Tau aggregated along microtubules in distal dendrites and on the SA and the postsynaptic membrane of presumed glutamatergic spine synapses, including evidence of vesicular trafficking in young axons and aged spines. In contrast, phosphorylated tau was not observed in aged primate V1, consistent with the pattern of NFT formation in AD. Although the distribution of pS214-tau in the aged monkey cortex resembles the pattern of NFT seen in AD, it is uncertain whether the process observed here is immediately relevant to NFT formation and degeneration in human disease. It is also likely that there are additional factors that contribute to increased tau phosphorylation in aging dlPFC, e.g., increased phosphorylation by other kinases (5) and reduced dephosphorylation by phosphatases (26). However, the loss of PDE4A with advancing age is an unexpected and important discovery. Future research may explore why PDE4A is lost from aged dendritic spines and whether treatments that inhibit Ca^{2+}-cAMP signaling in the spine can reduce p-tau expression in the aging cortex.

Species Differences. The great expansion in the number of corticocortical synapses on spines in primate dlPFC (27) likely makes it possible to detect the age-related loss of PDE4A from spines, as demonstrated with ImmunoEM, in whole tissue samples. In contrast, age-related changes in PDE4A in mouse PFC were detected only in the synaptosomal fraction, possibly due to the smaller number and volume proportion of spines in whole tissue. pS214-Tau was also not detected in whole mouse PFC, consistent with literature showing that normal mice are not appropriate for modeling AD (10). It is possible that a very small amount of pS214-tau could have been detected in isolated synapses; however, the methods required for isolating synapses are incompatible with those needed to accurately quantify p-tau. In contrast, the abundance of pS214-tau–containing spines as
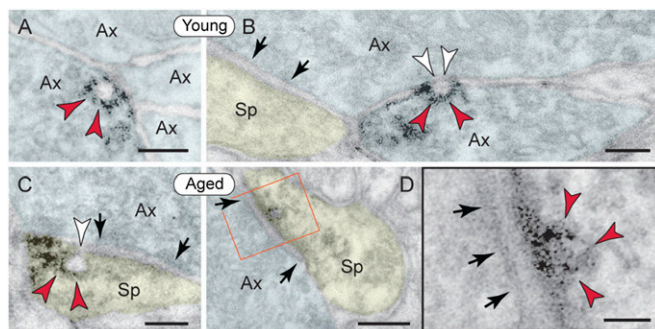
Fig. 3. Vesicular trafficking of pS214-tau in monkey dlPFC. (*A* and *B*) Axons in young dlPFC contained 60 nm p-tau–reactive vesicles (red arrowheads) that fused with the axolemma to form exocytotic omega-shaped profiles (*B*, white arrowheads). (*C* and *D*) In aged dlPFC, p-tau vesicular profiles (red arrowheads) were no longer present in axons but found in spines, fusing with the perisynaptic membrane flanking presumed glutamatergic synapses (*C*, white arrowhead), and within the synapse per se (*D*, *Inset*). Arrows point to asymmetric axospinous synapses. Ax, axon; Sp, spine. (Scale bars: *A–C*, 100 nm; *D*, 200 nm; and *D*, *Inset*, 50 nm.)
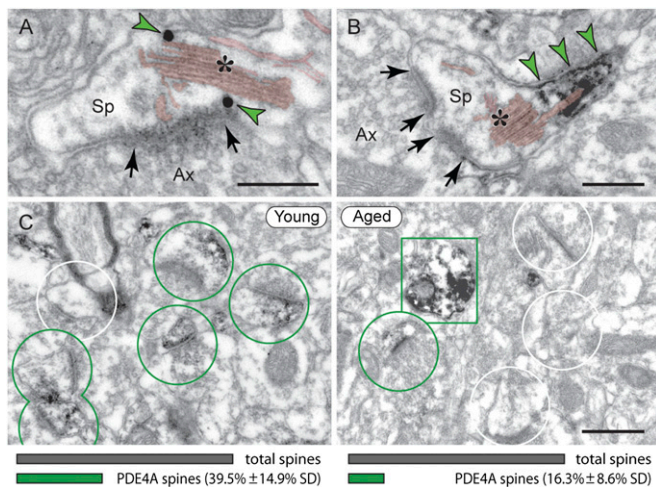
Fig. 4. PDE4A is lost from dendritic spines in aged monkey dlPFC. (*A* and *B*) In young dlPFC, PDE4A (green arrowheads) is localized next to the SA (asterisk); shown are immunogold and immunoperoxidase, respectively. (Scale bars: 200 nm.) (*C*) PDE4A is widely expressed in layer III spines in young, but not in aged monkey dlPFC (green circles, PDE4A spines; white circles, unlabeled spines; green rectangle, PDE4A dendrite). (Scale bar: 0.5 μm.) The graphs illustrate percentage of PDE4A spines in 10-y vs. 25-y monkey dlPFC (*Upper*), averaged from 46-μm² electron microscopic fields (20 fields from five tissue blocks per animal; *SI Materials and Methods*) of layer III. Young (*Left*): PDE4A spines/46 μm² = 5.95 (± 2.13 SD). Aged (*Right*): PDE4A spines/46 μm² = 2.05 (± 1.24 SD).

well as the extensive aggregation of pS214-tau in dendrites magnifies age-related increases in tau phosphorylation in monkey dlPFC. The vast expansion of corticocortical connections on dendritic spines through primate evolution may magnify this process further in human cortex and lead to sufficient phosphorylation to cause fibrillation, NFT formation, and neuronal degeneration. Thus, as association cortex evolves from rodents to monkeys to humans, there may be a parallel expansion in vulnerability to degeneration when dynamic modulation by cAMP-Ca^{2+} signaling becomes dysregulated with advancing age.

Relevance to Degeneration of Higher Cortical Circuits in AD. The discovery of p-tau aggregation at the spine postsynaptic membrane in aged primate dlPFC suggests that p-tau may interfere with synaptic transmission and receptor trafficking in pyramidal cell networks as part of normal aging, as has been seen in genetic rodent models (28, 29). This process may be exacerbated in individuals with tau mutations that promote phosphorylation (28, 29). Importantly, p-tau vesicles and aggregates were found only in asymmetric, presumed glutamatergic, axospinous synapses in aged dlPFC. These findings are consistent with the enrichment of p-tau in cortical synaptosome preparations from patients with AD (30) and illuminate how degeneration could specifically target those highly evolved glutamatergic pyramidal cell circuits that interconnect extensively on dendritic spines.

The presence of p-tau in endoplasmic vesicles fusing with the plasma membrane provides a possible mechanism for transneuronal lesion spread within pyramidal cell circuits in primate association cortex. Transneuronal spread of p-tau has recently been documented in genetically modified mouse AD models (31, 32), where it has been viewed as a route for "infection" of interconnected cortical circuits. However, evidence of p-tau trafficking has never before been documented in the normal aging brain and has never been captured with immunoEM. This study found striking differences between young and aged dlPFC, with p-tau vesicles exclusively in axons in young cortex vs. dendritic spines in the aged. The observation of p-tau trafficking in young axons is consistent with recent in vitro studies showing p-tau release during neuronal activity (33) and may also help to

explain why repeated head injury in young athletes leads to extensive axonal pathology in chronic traumatic encephalopathy (CTE) (34). The switch to spines in aged dlPFC suggests that axonal spread is concluded by the time p-tau aggregates in dendrites. p-Tau vesicular profiles in spines may indicate translocation within the spine, e.g., from and toward the postsynaptic membrane, as captured in Fig. 3 *C* and *D*, or possibly transneuronal transport.

It is possible that tau phosphorylation in both the spine and the dendrite are related events. For example, loss of PDE4A and p-tau accumulation on the SA may aggravate internal Ca^{2+} release sufficiently to spread through to the SER of the parent dendrite (35), where it may increase kinase phosphorylation of tau on microtubules. Aggregation of p-tau along the microtubules
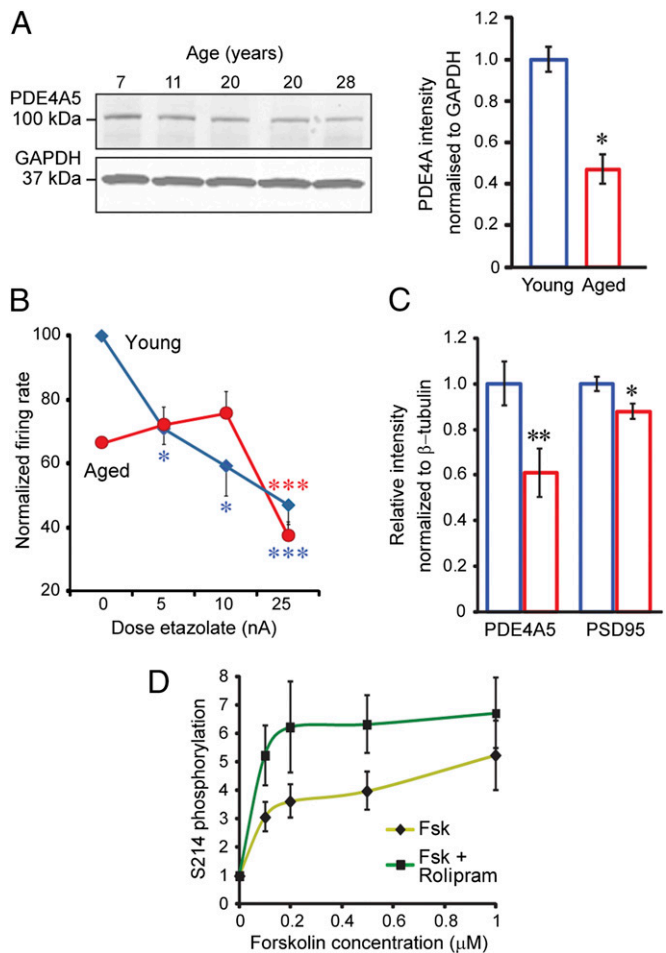
Fig. 5. PDE4A expression and physiological effect decrease with age in PFC. (*A*) Immunoblot and quantification of decreased PDE4A5 protein expression with age in monkey dlPFC, normalized to GAPDH, 7–11 y vs. 20–28 y, *$P < 0.05$. Individual data points in arbitrary units: 7 y = 0.93; 11 y = 1.06; 20 y = 0.61 and 0.38; and 28 y = 0.42. (*B*) Low doses of the PDE4 inhibitor etazolate (5–10 nA) decreased task-related firing of dlPFC neurons in young but not aged monkeys, whereas a high dose (25 nA) reduced firing in all neurons ($n = 39$). Shown are significant effects of dose ($F = 6.95$, $P = 0.002$) and age ($F = 12.27$, $P = 0.001$); significant changes from 0 nA, *$P < 0.05$, ***$P < 0.009$; and firing rates percentage of young control. (*C*) Quantification of postsynaptic density (PSD) preparations from mouse frontal cortex shows significant decrease of PDE4A5 in the PSD fraction with age, **$P < 0.05$, which remains significant ($P < 0.05$) when normalized by PSD95 levels to account for presumed spine loss. (*D*) PDE4 inhibitor, rolipram, increased pS214-tau in mouse primary cortical neurons. Activation of PKA by forskolin (Fsk) produced a dose-related increase in pS214-tau [$F(4,60) = 8.920$, $P < 0.0001$] that was significantly increased by rolipram [10 μM; $F(1,60) = 8.882$, $P = 0.0042$].
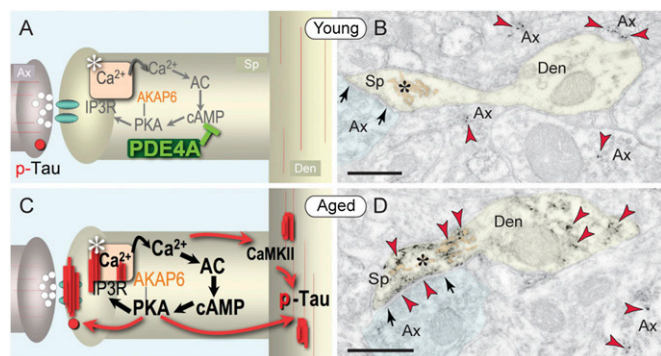
Fig. 6. Synopsis of age-related alterations in layer III corticocortical network synapses in primate dlPFC. (*A*) Schematic illustration of young dlPFC, with PDE4A positioned to regulate feedforward cAMP-Ca^{2+}-K$^+$ signaling near NMDAR glutamate synapses in dendritic spines (K$^+$ channels near synapse not shown). pS214-Tau is distributed sparsely along axonal and dendritic microtubules and in trafficking vesicles in axons (red circle). (*B*) Representative immunoEM of pS214-tau (red arrowheads) in young dlPFC. (*C*) Schematic illustration of changes in aged dlPFC, with loss of PDE4A, dysregulation of cAMP-Ca^{2+}-K$^+$ signaling, and aggregation of pS214-tau in the synapse and the SA (asterisk) and along microtubules in distal dendrites. pS214-Tau endoplasmic vesicles are no longer present in axons but appear in spines perisynaptically and within the synapse. (*D*) Representative immunoEM of pS214-tau in aged dlPFC. Ax, axon; Den, dendrite; Sp, spine; arrows point to asymmetric axospinous synapses. (Scale bars: 200 nm.)

of thin, highly branched dendrites may in turn cause steric hindrance, interfering with intracellular transport and thus injuring the neuron before NFTs are formed.

Potential Interactions with Aβ. p-Tau aggregation on dendritic microtubules may also interfere with trafficking of amyloid precursor protein (APP) and thus contribute to the production of Aβ. APP traffics in vesicles in distal pyramidal dendrites (36). When trafficking is disrupted, e.g., by genetic mutations in the retromer complex, APP is cleaved by beta-secretase 1 (BACE1) in the vesicular membrane to produce Aβ (36). A similar exacerbation of Aβ production may occur if APP trafficking is hindered by aggregated p-tau along the microtubules in aging. As Aβ oligomers drive intracellular Ca^{2+} release through stimulation of mGlu5 receptors on spines (37, 38), a vicious cycle could propel the degenerative process. Pathological signaling could be initiated at many points within the vicious cycle (e.g., increased Aβ due to genetic insults in APP processing or increased p-tau due to head injury and/or aging) and lead to a similar, degenerative phenotype.

Risk Factors for AD Increase cAMP-Ca^{2+} Signaling in PFC. Our data help to explain why aging is the highest risk factor for degeneration of pyramidal cell circuits in association cortex in AD and related disorders (1). Loss of PDE4A from spines with advancing age leads to dysregulation of cAMP-Ca^{2+} signaling and increased kinase phosphorylation of tau in pyramidal cell circuits. However, it has long been appreciated that head injury is also a significant risk factor for AD (39) as well as CTE (34, 40). More recently, psychological trauma has been identified as a risk factor for AD as well (41). All three of these factors—aging (23, 24), head trauma (42), and psychological trauma (43)—increase cAMP-Ca^{2+} signaling in PFC, thus providing a coherent explanation for how they all exacerbate the degenerative process.

Relevance to Prevention of AD. It is now appreciated that tau phosphorylation in humans begins relatively early in the aging process (2), suggesting that interventions need to be initiated at younger ages. The current study demonstrates that the aging monkey can serve as an important animal model for understanding the molecular events that render the association cortices especially vulnerable to degeneration and an opportunity to test agents that may slow or

prevent this process by compensating for PDE4A dysregulation of cAMP signaling in dendritic spines. This strategy would complement existing research focused on genetic mouse models and target the unique vulnerabilities of the highly evolved brain circuits most susceptible to degeneration.

Materials and Methods

All procedures were approved by the Yale Institutional Animal Care and Use Committee.

Tissue Processing for ImmunoEM. Three young adult (9–11 y) and five aged (24–26 y, 29 y, and 31 y) rhesus macaques were perfused transcardially with artificial cerebrospinal fluid, followed by 4% (wt/vol) paraformaldehyde/0.05% glutaraldehyde, plus 0.2% picric acid in 0.1 M phosphate buffer (PB). The brains were blocked coronally, vibrosliced at 60 μm, cryoprotected, and stored at −80 °C. Sections of the dlPFC went through three freeze–thaw cycles in liquid nitrogen to facilitate penetration of immunoreagents and were processed free-floating for immunocytochemistry.

Single and Dual Immunocytochemistry. For single labeling, sections were incubated for 36 h in rabbit anti-PDE4A IgG (1:300; ab14607; Abcam) or mouse anti-pS214-tau (CP3) IgM (1:100) (4) or mouse anti-AKAP6 IgG2 (1:200; SAB1401476; Sigma-Aldrich), followed by species-specific biotinylated secondary antibodies (Jackson Immunoresearch) and the avidin-biotinylated peroxidase reaction using DAB as a chromogen. Alternatively, secondaries were conjugated to 1.4 nm gold cluster (Nanoprobes) and visualized with silver intensification of gold (compare Fig. 4*A* to 4*B*). The procedures and immunoprobes are described in detail in ref. 20.

For dual immunolabeling, sections were incubated for 48 h in a mixture of anti-PDE4A and anti-AKAP6 (see above). Biotinylated and 1.4 nm gold-conjugated species-specific secondary antibodies were used to label PDE4A with DAB, as described for single labeling, and AKAP6 with silver-intensified gold; see ref. 20 for the detailed dual immunoprocedure and methodological controls.

Electron Microscopy and Data Analysis. Labeled tissue was processed for electron microscopy, using 40-nm-thick plastic sections and omitting counterstaining to facilitate weak signal detection. Quantitative analyses were performed on series of low-magnification images, each capturing a field of 46 μm^2. A comprehensive account of tissue sampling and data collection is described in *SI Materials and Methods*. Micrographs were edited using Photoshop CS4 (Adobe Systems) for brightness and contrast (applied to the entire panel) and pseudocolored for clarity. No other manipulation was made to raw images.

Single Neuron Recording and Iontophoresis. Studies were performed on two young adult (9 y and 10 y) and one aged (21 y) rhesus macaques trained on the spatial oculomotor delayed response task (Fig. S5). MRI confirmed recording within a region ~1–2 mm medial and ~0–3 mm anterior to the caudal end of the principal sulcus. Iontophoretic electrodes were constructed with 20 μm pitch carbon fiber inserted in the central barrel of seven-barrel capillary glass. Signals were digitized and acquired using Spike2 software. The Neurophore BH2 iontophoretic system controlled delivery of the drugs. Etazolate hydrochloride (Tocris) was dissolved at 0.01 M in triple-distilled water (pH 3.5–4.0). Two-way ANOVA was used to examine the spatially tuned delay-related activity with regard to task periods (fixation vs. delay) and cue locations, and one-way ANOVA was used to assess the effect of drug on delay-related activity. The equipment and procedures have been described in detail previously (12, 13).

Heat-Stable Tau Preparations. Heat-stable tau was prepared as detailed in ref. 44. Blocks of monkey dlPFC were surgically removed and flash-frozen before aldehyde perfusion. Tissue was placed into ice-cold homogenization buffer (400 μL per 100 mg tissue) and homogenized by sonication; a fraction was reserved for protein quantification for gel loading. NaCl was added to 250 mM, followed by 14.3 M β-mercaptoethanol to 5% total volume. Samples were vortexed, heated to 100 °C for 15 min, vortexed, and cooled for 30 min on ice. Lysates were cleared, and the supernatant was used for immunoblotting. Tau band intensities were normalized by total heat-stable protein, quantified from whole-lane intensity on a Coomassie-stained gel.

Immunoblots. Primary antibodies were visualized using the appropriate Licor IRDye 680 or 800 secondaries and a Licor Odyssey Infra Red Scanner. Bands were quantified with Odyssey Software, and statistics were performed by Student's *t*-test, unless stated otherwise. Antibody information is given in Figs. S2, S6, and S9.

Postsynaptic Density Preparations. Mice were decapitated, and the frontal cortex was dissected into 1 mL of homogenization buffer [20 mM Hepes (pH 7.4), 0.32 M sucrose, protease, and phosphatase inhibitors]. Two cortical sections were pooled to provide ~100 mg of tissue. Synaptoneurosomes were prepared as in ref. 45. The interface between the 15% and 23% layers was pooled with the interface between the 10% and 15% fractions. Pellets were hypotonically lysed [20 mM Hepes (pH 7.4), 1 mM DTT, protease, and phosphatase inhibitors] for 30 min on ice. The sample was collected by centrifugation and the pellet resuspended in 2 mL of Triton buffer [20 mM Hepes (pH 7.4), 0.32 M sucrose, 0.75% Triton X-100] for 15 min to extract Triton-insoluble postsynaptic densities, which were collected by ultracentrifugation and resuspended in PBS with 1% SDS.

cAMP Assays. cAMP levels were measured in the medial PFC of seven young adult (6 mo) and four aged (24 mo) Brown Norway rats. Rats were killed by focused microwave radiation and the brains rapidly removed and frozen. Tissue was dissected and sonicated in 0.1 M HCl/0.5% Triton X-100 on ice, and samples were cleared by centrifugation. Supernatants were used for cAMP assays, using the Correlate-EIA Enzyme Immunoassay Kit (Assay Designs). All samples and standards were run in duplicate, and results were averaged. Concentrations were determined by reference to a standard curve, and estimates (pmole cAMP) were divided by tissue mass. Data were analyzed by one-way ANOVA.

Primary Cortical Neuron Culture. Primary cortical neurons were prepared from P1 C57BL/6 mice. Brains were dissected in buffer (HBSS, L-glutamine, 7 mM Hepes; GIBCO). Cortices were microdissected and the hippocampi

discarded. Tissue was then transferred to 0.1% trypsin solution and incubated for 45 min before trituration and filtration (40 μM) to a single-cell suspension. Cells were plated at a density of 5×10^5 live cells per well (six-well plates) in Neurobasal media plus B27 supplement, Glutamax, and Pen/Strep solution. Cells were incubated at 37 °C, 5% CO_2, with media replenished every 7 d.

pS214 Phosphorylation Assays in Cultured Neurons. Assays were performed on mouse primary cortical neurons (7–11 d in vitro). Cells were preincubated with vehicle or 10 μM rolipram in DMSO (Sigma) for 10 min and treated with increasing concentrations of forskolin (Abcam; 100 nM, 200 nM, 500 nM, and 1,000 nM in DMSO), in the presence or absence of 10 μM rolipram for a further 10 min. Cells were lysed in PBS with 1% SDS, plus protease and phosphatase inhibitors, and heated to 70 °C for 10 min to inactivate phosphatases. Samples were quantified by bicinchoninic acid assay and analyzed by immunoblotting. Band intensity was quantified using ImageJ and significance assessed by two-way ANOVA, using Graph Pad Prism.

1. Evans DA, et al. (1989) Prevalence of Alzheimer's disease in a community population of older persons. Higher than previously reported. *JAMA* 262(18):2551–2556.
2. Braak H, Thal DR, Ghebremedhin E, Del Tredici K (2011) Stages of the pathologic process in Alzheimer disease: Age categories from 1 to 100 years. *J Neuropathol Exp Neurol* 70(11):960–969.
3. Giannakopoulos P, et al. (2003) Tangle and neuron numbers, but not amyloid load, predict cognitive status in Alzheimer's disease. *Neurology* 60(9):1495–1500.
4. Jicha GA, et al. (1999) cAMP-dependent protein kinase phosphorylations on tau in Alzheimer's disease. *J Neurosci* 19(17):7486–7494.
5. Sengupta A, et al. (1998) Phosphorylation of tau at both Thr 231 and Ser 262 is required for maximal inhibition of its binding to microtubules. *Arch Biochem Biophys* 357(2):299–309.
6. Sengupta A, Grundke-Iqbal I, Iqbal K (2006) Regulation of phosphorylation of tau by protein kinases in rat brain. *Neurochem Res* 31(12):1473–1480.
7. Pearson RC, Esiri MM, Hiorns RW, Wilcock GK, Powell TP (1985) Anatomical correlates of the distribution of the pathological changes in the neocortex in Alzheimer disease. *Proc Natl Acad Sci USA* 82(13):4531–4534.
8. Lewis DA, Campbell MJ, Terry RD, Morrison JH (1987) Laminar and regional distributions of neurofibrillary tangles and neuritic plaques in Alzheimer's disease: A quantitative study of visual and auditory cortices. *J Neurosci* 7(6):1799–1808.
9. Bussière T, et al. (2003) Progressive degeneration of nonphosphorylated neurofilament protein-enriched pyramidal neurons predicts cognitive impairment in Alzheimer's disease: Stereologic analysis of prefrontal cortex area 9. *J Comp Neurol* 463(3):281–302.
10. Platt TL, Reeves VL, Murphy MP (2013) Transgenic models of Alzheimer's disease: Better utilization of existing models through viral transgenesis. *Biochim Biophys Acta* 1832(9):1437–1448.
11. Goldman-Rakic PS (1995) Cellular basis of working memory. *Neuron* 14(3):477–485.
12. Wang M, et al. (2013) NMDA receptors subserve persistent neuronal firing during working memory in dorsolateral prefrontal cortex. *Neuron* 77(4):736–749.
13. Yang Y, et al. (2013) Nicotinic α7 receptors enhance NMDA cognitive circuits in dorsolateral prefrontal cortex. *Proc Natl Acad Sci USA* 110(29):12078–12083.
14. Arnsten AF, Wang MJ, Paspalas CD (2012) Neuromodulation of thought: Flexibilities and vulnerabilities in prefrontal cortical network synapses. *Neuron* 76(1):223–239.
15. Paspalas CD, Goldman-Rakic PS (2004) Microdomains for dopamine volume neurotransmission in primate prefrontal cortex. *J Neurosci* 24(23):5292–5300.
16. Soulsby MD, Wojcikiewicz RJ (2005) The type III inositol 1,4,5-trisphosphate receptor is phosphorylated by cAMP-dependent protein kinase at three sites. *Biochem J* 392(Pt 3):493–497.
17. Liu X, et al. (2012) Role of leaky neuronal ryanodine receptors in stress-induced cognitive dysfunction. *Cell* 150(5):1055–1067.
18. Ferguson GD, Storm DR (2004) Why calcium-stimulated adenylyl cyclases? *Physiology* 19:271–276.
19. Kapiloff MS, Rigatti M, Dodge-Kafka KL (2014) Architectural and functional roles of A kinase-anchoring proteins in cAMP microdomains. *J Gen Physiol* 143(1):9–15.
20. Paspalas CD, Wang M, Arnsten AF (2013) Constellation of HCN channels and cAMP regulating proteins in dendritic spines of the primate prefrontal cortex: Potential substrate for working memory deficits in schizophrenia. *Cereb Cortex* 23(7):1643–1654.
21. Mattson MP (2007) Calcium and neurodegeneration. *Aging Cell* 6(3):337–350.
22. Oh MM, Oliveira FA, Waters J, Disterhoft JF (2013) Altered calcium metabolism in aging CA1 hippocampal pyramidal neurons. *J Neurosci* 33(18):7905–7911.

23. Ramos BP, et al. (2003) Dysregulation of protein kinase a signaling in the aged prefrontal cortex: New strategy for treating age-related cognitive decline. *Neuron* 40(4):835–845.
24. Wang M, et al. (2011) Neuronal basis of age-related working memory decline. *Nature* 476(7359):210–213.
25. Liang WS, et al. (2007) Gene expression profiles in anatomically and functionally distinct regions of the normal aged human brain. *Physiol Genomics* 28(3):311–322.
26. Braithwaite SP, Stock JB, Lombroso PJ, Nairn AC (2012) Protein phosphatases and Alzheimer's disease. *Prog Mol Biol Transl Sci* 106:343–379.
27. Elston GN, et al. (2006) Specializations of the granular prefrontal cortex of primates: Implications for cognitive processing. *Anat Rec A Discov Mol Cell Evol Biol* 288(1):26–35.
28. Hoover BR, et al. (2010) Tau mislocalization to dendritic spines mediates synaptic dysfunction independently of neurodegeneration. *Neuron* 68(6):1067–1081.
29. Hochgräfe K, Sydow A, Mandelkow EM (2013) Regulatable transgenic mouse models of Alzheimer disease: Onset, reversibility and spreading of Tau pathology. *FEBS J* 280(18):4371–4381.
30. Sokolow S, et al. (2012) Isolation of synaptic terminals from Alzheimer's disease cortex. *Cytometry A* 81(3):248–254.
31. de Calignon A, et al. (2012) Propagation of tau pathology in a model of early Alzheimer's disease. *Neuron* 73(4):685–697.
32. Liu L, et al. (2012) Trans-synaptic spread of tau pathology in vivo. *PLoS ONE* 7(2):e31302.
33. Pooler AM, Phillips EC, Lau DH, Noble W, Hanger DP (2013) Physiological release of endogenous tau is stimulated by neuronal activity. *EMBO Rep* 14(4):389–394.
34. McKee AC, et al. (2013) The spectrum of disease in chronic traumatic encephalopathy. *Brain* 136(Pt 1):43–64.
35. Volfovsky N, Parnas H, Segal M, Korkotian E (1999) Geometry of dendritic spines affects calcium dynamics in hippocampal neurons: Theory and experiments. *J Neurophysiol* 82(1):450–462.
36. Bhalla A, et al. (2012) The location and trafficking routes of the neuronal retromer and its role in amyloid precursor protein transport. *Neurobiol Dis* 47(1):126–134.
37. Renner M, et al. (2010) Deleterious effects of amyloid beta oligomers acting as an extracellular scaffold for mGluR5. *Neuron* 66(5):739–754.
38. Um JW, et al. (2013) Metabotropic glutamate receptor 5 is a coreceptor for Alzheimer aβ oligomer bound to cellular prion protein. *Neuron* 79(5):887–902.
39. Guo Z, et al. (2000) Head injury and the risk of AD in the MIRAGE study. *Neurology* 54(6):1316–1323.
40. Blennow K, Hardy J, Zetterberg H (2012) The neuropathology and neurobiology of traumatic brain injury. *Neuron* 76(5):886–899.
41. Johansson L, et al. (2013) Common psychosocial stressors in middle-aged women related to longstanding distress and increased risk of Alzheimer's disease: A 38-year longitudinal population study. *BMJ Open* 3(9):e003142.
42. Kobori N, Hu B, Dash PK (2011) Altered adrenergic receptor signaling following traumatic brain injury contributes to working memory dysfunction. *Neuroscience* 172:293–302.
43. Arnsten AF (2009) Stress signalling pathways that impair prefrontal cortex structure and function. *Nat Rev Neurosci* 10(6):410–422.
44. Giliberto L, d'Abramo C, Acker CM, Davies P, D'Adamio L (2010) Transgenic expression of the amyloid-beta precursor protein-intracellular domain does not induce Alzheimer's Disease-like traits in vivo. *PLoS ONE* 5(7):e11609.
45. Dunkley PR, Jarvie PE, Robinson PJ (2008) A rapid Percoll gradient procedure for preparation of synaptosomes. *Nat Protoc* 3(11):1718–1728.

NEUROSCIENCE